ISSN 1063-7761, Journal of Experimental and Theoretical Physics, 2010, Vol. 111, No. 2, pp. 189–193. © Pleiades Publishing, Inc., 2010.
Original Russian Text © N.A. Babushkina, A.N. Taldenkov, A.V. Kalinov, L.M. Fisher, O.Yu. Gorbenko, T. Lorenz, D.I. Khomskii, K.I. Kugel', 2010, published in Zhurnal Éksperimental'noĭ i Teoreticheskoĭ Fiziki, 2010, Vol. 138, No. 2, pp. 215–220.

ORDER, DISORDER, AND PHASE TRANSITION IN CONDENSED SYSTEM

Isotope Effect and Characteristic Features of the Phase Diagram for Cobaltites with Spin-State Transitions

N. A. Babushkina[a], A. N. Taldenkov[a,*], A. V. Kalinov[b], L. M. Fisher[b], O. Yu. Gorbenko[c†], T. Lorenz[d], D. I. Khomskii[d], and K. I. Kugel'[e]

[a] *Russian Research Centre Kurchatov Institute, pl. Akademika Kurchatova 1, Moscow, 123182 Russia*
**e-mail: taldenkov@imp.kiae.ru*
[b] *All-Russia Electrical Engineering Institute, Krasnokazarmennaya ul. 12, Moscow, 111250 Russia*
[c] *Moscow State University, Moscow, 119991 Russia*
[d] *II. Physikalisches Institut, Universität zu Köln, Zülpicher Str. 77, Köln, 50937 Germany*
[e] *Institute for Theoretical and Applied Electrodynamics, Russian Academy of Sciences, Izhorskaya ul. 13, Moscow, 125412 Russia*

Received October 30, 2009

Abstract—The effect of $^{16}O \longrightarrow {}^{18}O$ oxygen isotope substitution has been studied for $(Pr_{1-y}Eu_y)_{0.7}Ca_{0.3}CoO_3$ cobaltites ($0.12 < y < 0.26$). A pronounced isotope shift has been found for the spin-state transition temperature, which increases with the oxygen isotope mass. In contrast, the ferromagnetic transition temperature has slightly lower values for the samples with heavier oxygen. The observed phenomena and constructed phase diagram confirm the results reported previously for $(Pr_{1-y}Sm_y)_{0.7}Ca_{0.3}CoO_3$ in [G. Y. Wang, X. H. Chen, T. Wu, et al., Phys. Rev. B **74**, 165113 (2006)]. The measurements of the specific heat have been performed for $(Pr_{1-y}Eu_y)_{0.7}Ca_{0.3}CoO_3$ with the main emphasis on the analysis of the isotope effect. The contributions to the isotope effect coming from the lattice and magnetic components of the specific heat have been separated. The mechanisms underlying the large isotope effect are discussed.

DOI: 10.1134/S1063776110080042

1. INTRODUCTION

The isotope substitution is an efficient tool for the study of lattice dynamics, as well as the electrical and magnetic properties of solids. In some cases, particularly if a system is close to the crossover between different states, the isotope substitution can lead to significant changes in the ground state of the system. In manganites, for example, a metal–insulator transition induced by the $^{16}O \longrightarrow {}^{18}O$ isotope substitution was observed [1].

Complex cobalt oxides $ACoO_3$ with the perovskite-type structure attract a significant current interest [2–4]. Position A in the cobaltite lattice is usually occupied by a combination of rare-earth and alkaline-earth elements. The variations in the content of alkaline-earth elements, in particular Ca, give rise to changes in the charge carrier density. The combination of different rare-earth elements allows for a fine tuning of the lattice structure by slightly changing the average ionic radius in the course of isovalent doping.

An interesting feature of cobaltites is the possibility of a transition involving the change in the spin state of the Co^{3+} ion. With an increase in the temperature, these compounds undergo a spin-state (SS) transition at $T = T_{SS}$ from the low-spin ground state (LS, $t_{2g}^6 e_g^0$, $S = 0$) to the intermediate-spin (IS, $t_{2g}^5 e_g^1$, $S = 1$) or high-spin (HS, $t_{2g}^4 e_g^2$, $S = 2$) state. It turns out that the ionic radius of the cobalt ion in the intermediate-spin and high-spin states is larger than that for the low-spin state of Co^{3+} ($S = 0$), Hence, the spin-state transition is accompanied by a significant reconfiguration in the cobaltite lattice. Alongside with these changes, the transition to the low-spin state manifests itself in a significant decrease in the electrical conductivity; the corresponding increase in the resistance can be as large as several orders of magnitude. This allows us to treat such a phenomenon as a metal–insulator transition [5]. Such interplay between magnetic, lattice, and charge degrees of freedom can result in the pronounced isotope effect.

Indeed, the measurements reported in [6, 7] demonstrated the giant oxygen isotope effect in $(Pr_{1-y}Sm_y)_{0.7}Ca_{0.3}CoO_3$ cobaltites. It was found that small variations in the ionic radius due to the isovalent substitution of samarium for praseodymium give rise to significant changes in the magnetic structure of this compound and even to the complete change of the ground state. In this case, the oxygen isotopic parameter (power-law exponent) $\alpha_O = \partial \ln T_{SS} / \partial \ln(M_O)$

† Deceased.

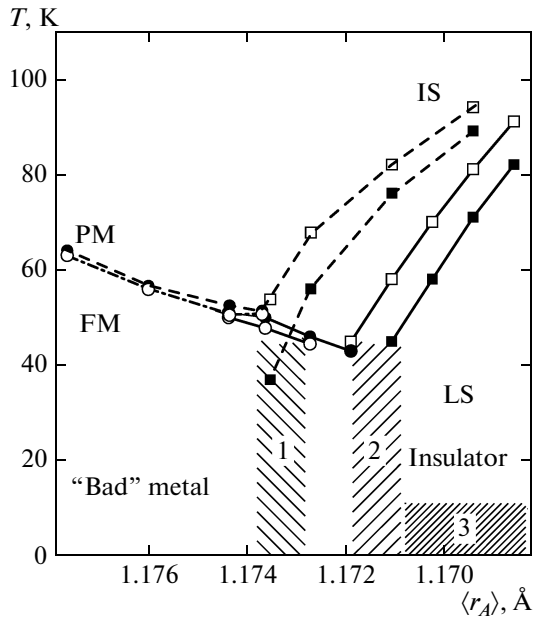

Fig. 1. Phase diagram of $ACoO_3$ cobaltites in the plane temperature versus the average ionic radius $\langle r_A \rangle$ of a cation in the A position (according to the results reported in [7, 8]). The solid and dashed lines correspond to $(Pr_{1-y}Eu_y)_{0.7}Ca_{0.3}CoO_3$ and $(Pr_{1-y}Sm_y)_{0.7}Ca_{0.3}CoO_3$, respectively. The squares and circles denote spin-state and ferromagnetic transitions, respectively. The filled and open symbols correspond to the samples enriched in ^{18}O and ^{16}O, respectively. The prevailing spin states of cobalt ions (PM, FM, IS, and LS) are indicated. Hatched areas 1 and 2 mark the crossover regions in the vicinity of $y = y_c$ for $(Pr_{1-y}Sm_y)_{0.7}Ca_{0.3}CoO_3$ and $(Pr_{1-y}Eu_y)_{0.7}Ca_{0.3}CoO_3$, respectively. Hatched area 3 corresponds to the region of low-temperature ferromagnetic ordering in $(Pr_{1-y}Eu_y)_{0.7}Ca_{0.3}CoO_3$ according to the data reported in [8].

(M_O is the average atomic mass of oxygen) has an anomalously large value $\alpha_O \gg 0.5$ near the threshold value $y_c \approx 0.175$ characterized by the competition between the ferromagnetic metallic and weakly magnetic insulating states favoring the phase separation. Note that α_O corresponding to the ferromagnetic (FM) transition is small and its sign is opposite to that for the spin-state transition.

Recently [8], we reported a detailed study of $(Pr_{1-y}Eu_y)_{0.7}Ca_{0.3}CoO_3$ cobaltite within the $0.12 < y < 0.26$ concentration range. It was shown that an increase in Eu content (leading to an increase in static lattice distortions) results in the change of the ground state from the ferromagnetic semimetal to the weakly magnetic semiconductor (insulator). The spin-state transition arises in the $(Pr_{1-y}Eu_y)_{0.7}Ca_{0.3}CoO_3$ system at $y_c > 0.18$. Using the magnetic, electrical, and thermal data, we constructed a phase diagram for this material, analyzed the possible charge and magnetic states of cobalt ions, and confirmed the existence of the giant isotope effect in the $(Pr_{1-y}Eu_y)_{0.7}Ca_{0.3}CoO_3$ system. The characteristic feature of this phase diagram is a broad crossover range near the concentration $y_c \approx 0.18$, dividing the phase plane into the regions with high and low europium contents [8].

Figure 1 shows the joint phase diagram for $(Pr_{1-y}Sm_y)_{0.7}Ca_{0.3}CoO_3$ and $(Pr_{1-y}Eu_y)_{0.7}Ca_{0.3}CoO_3$ cobaltites versus the average ionic radius $\langle r_A \rangle$ in position A based on the results reported in [7, 8]. In general, the diagrams of both compounds are similar to each other with the only difference that the phase boundary corresponding to the spin-state transition in the Eu-containing compound is shifted toward larger values of the ionic radius. The nature of such a difference is not quite clear now. The values of the isotope shift for the temperatures of ferromagnetic, spin-state, and metal–insulator transitions are nearly the same for both compounds.

In [8], we analyzed the thermal, magnetic, and electrical measurements and drew certain conclusions concerning the spin state of cobalt ions. It was shown that the compositions with a low Eu content at $T < T_{FM}$ correspond to the domains of the metallic ferromagnetic phase embedded in a weakly magnetic nonconducting matrix. However, even in the paramagnetic (PM) state ($T > T_{FM}$), Co^{3+} ions can occur in both the intermediate-spin and low-spin states. The paramagnetic–ferromagnetic transition is not accompanied by significant changes in the electrical conductivity. An increase in the Eu(Sm) content stabilizes the low-spin state of Co^{3+} but, as was mentioned on [8], only a part of Co^{3+} ions undergo the spin-state transition upon cooling. The spin-state transition is accompanied by the metal–insulator transition. At extremely low temperatures, the ferromagnetic state related to the partial spin ordering of Co^{4+} ions can appear. Within the crossover concentration range near y_c, there exists a broad phase-separation region.

The aim of this work is to study the manifestation of the isotope effect in thermal (such as the specific heat) properties of $(Pr_{1-y}Eu_y)_{0.7}Ca_{0.3}CoO_3$ cobaltites ($0.12 < y < 0.26$).

2. EXPERIMENTAL TECHNIQUES AND THE SAMPLES

Ceramic samples of $(Pr_{1-y}Eu_y)_{0.7}Ca_{0.3}CoO_3$ cobaltites were produced in the form of pellets by the solid-phase "paper" synthesis. The synthesis technique is described in detail in [8]. At the final stage of their production, the pellets were sintered at $T = 1000°C$ for 100 h. In the produced samples, the $^{16}O \longrightarrow {}^{18}O$ oxygen isotope substitution was performed. Two rectangular samples cut from the same pellet of the initial material were simultaneously annealed for 200 h at a temperature of $T = 950°C$ and a pressure of $p = 1$ bar, each in its own gas atmosphere, namely in $^{16}O_2$ and $^{18}O_2$ (enrichment up to 93% of ^{18}O). The enrichment

of the sample in ^{18}O was determined by the weight change and was equal to about 92%. In total, eight pairs of $(Pr_{1-y}Eu_y)_{0.7}Ca_{0.3}CoO_3$ samples with different y values were prepared. The similarity of the oxygen isotope composition in the sample to that in the gas medium indicated that the thermal equilibrium was achieved during the annealing process. Note also that the mass of a sample annealed in $^{16}O_2$ remained unchanged within the experimental error during the prolonged heat treatment. Thus, we can conclude that the used annealing procedure does not change the oxygen stoichiometry in the compounds under study. The X-ray diffraction analysis demonstrated the single-phase state of the samples. The specific heat was measured using a Quantum Design PPMS instrument by the two-tau relaxation technique.

3. RESULTS AND DISCUSSION

The temperature dependence of the specific heat $C_P(T)/T$ for the samples with the compositions from the phase diagram regions corresponding to high and low Eu contents is shown in Fig. 2 along with the specific heat of the nonmagnetic $Eu_{0.7}Ca_{0.3}Co^{16}O_3$ sample containing Co^{3+} in the low-spin state [8]. The latter sample is used as a reference isostructural analog of the compound with the pure phonon specific heat at $T >$ 10 K. The observed features in C_P/T indicate the spin-state transitions for the samples with $y = 0.22$ and 0.26. The isotope shift of the spin-state transition point is clearly seen. At very low temperatures, an increase in C_P/T is observed. The detailed analysis of the temperature and magnetic field dependences of the specific heat performed in [8] demonstrated that this increase is due to the arising ferromagnetic ordering in the dilute system of Co^{4+} ions in the nonmagnetic matrix formed by the low-spin Co^{3+} ions. A similar interpretation is also valid for the specific heat of the $Eu_{0.7}Ca_{0.3}Co^{16}O_3$ sample. The temperature dependence of the specific heat for the sample with a low Eu content ($y = 0.14$) does not exhibit a peak corresponding to the spin-state transition. A shoulder corresponding to the absence of a pronounced phase transition in the presence of competing types of exchange interaction is instead observed in a wide temperature range below 100 K. It can be assumed that the lattice contribution to the specific heat is the same, whereas the magnetic contributions to the specific heat reproduce the characteristic features of the ordering for Co ions in different spin states. Note that the specific heat at high temperatures is determined mostly by phonons (C_{lat}) and the specific heat plots for ^{18}O-enriched samples at these temperatures lie systematically higher than those corresponding to the samples with the lighter oxygen isotope.

To analyze the isotope effect in the specific heat, the logarithmic derivative of the specific heat with respect to the isotope mass of the ith element $\beta_i = \partial\ln(C_V/T^3)/\partial\ln M_i$ or its finite-difference representation determined from the experimental data, $\beta_i = \Delta C_P M_i/C_P\Delta M_i$, is commonly used. The β_i value can be found both for each kind of atoms (i) with the average mass M_i and for the unit cell as a whole having mass M. The specific heat C_P is assumed to be close to C_V according to the estimate given in [9]. For the lattice specific heat, β_i is always positive. In the low-temperature limit of the Debye model, it can be written as $\beta_i = 3M_i/2M$.

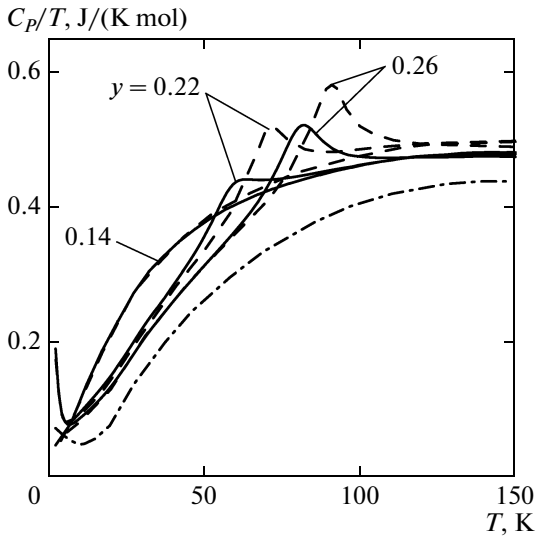

Fig. 2. Temperature dependence of the specific heat for (solid lines) $(Pr_{1-y}Eu_y)_{0.7}Ca_{0.3}Co^{16}O_3$, (dashed lines) $(Pr_{1-y}Sm_y)_{0.7}Ca_{0.3}Co^{18}O_3$, and (dash–dotted lines) $Eu_{0.7}Ca_{0.3}Co^{16}O_3$ samples.

Figure 3 shows the temperature dependence of the coefficient β_O for the ^{16}O and ^{18}O oxygen isotopes, calculated using the experimental data for the specific heat (see Fig. 2). Since the high-temperature values of the specific heat are close to those given by the Dulong–Petit law, $C_V = 15R = 125$ J/(K mol), we can conclude that $C \approx C_{lat}$ and nearly all of the acoustic and optical phonon modes are excited. In this situation, the value of β_O should decrease down to zero with an increase in the temperature near the Debye temperature T_D and the characteristic temperatures T_E corresponding to the Einstein modes. To estimate the isotope effect in C_{lat}, let us use a simple representation for the specific heat as a sum of the Einstein $E(T_E)$ and Debye $D(T_D)$ functions

$$C_{lat} \propto D(T_D) + E(T_E). \quad (1)$$

Assuming that $T_D \propto M^{-1/2}$ and $T_E \propto M_O^{-1/2}$, it is possible to obtain a good high-temperature fit for the experimental $\beta_O(T)$ plot (see Fig. 3) using the values $T_E = 500$ K and $T_D = 630$ K, which are close to the published data (see, e.g., [9]). With a decrease in the temperature, the calculated value of $\beta_O(T)$ becomes substantially larger than the experimental values due

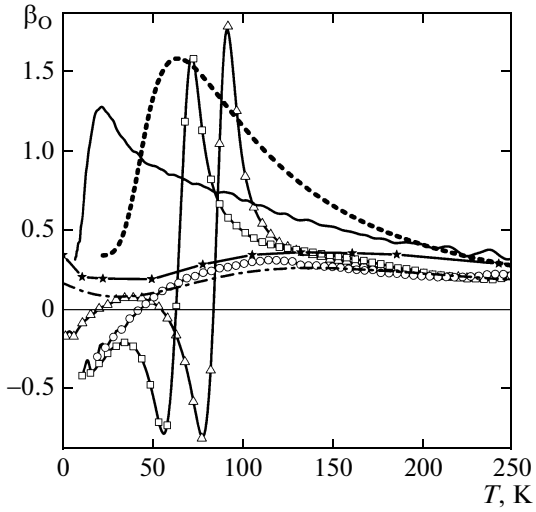

Fig. 3. Temperature dependence of the oxygen isotope parameter β_O for $(Pr_{1-y}Eu_y)_{0.7}Ca_{0.3}CoO_3$ with $y =$ (triangles) 0.26, (squares) 0.22, and (circles) 0.14. The stars are the experimental data for ZnO [10]. The symbols are connected by solid lines. The solid, dashed, and dash–dotted lines correspond to the calculations by Eqs. (1), (2), and for ZnO [10], respectively.

to the exponential temperature dependence characteristic of the Einstein function.

Another method to estimate $\beta_O(T)$ is to use the well-known relation

$$\beta = \frac{\partial \ln(C_V/T^3)}{\partial \ln M} = \frac{1}{2}\left(\frac{\partial \ln(C_V/T^3)}{\partial \ln T} + 3\right), \qquad (2)$$

which is well verified for monatomic solids, but also gives a quite precise estimate for $\beta(T)$ in diatomic crystals [10–12]. Using the $C_P(T)$ values measured for $Eu_{0.7}Ca_{0.3}Co^{16}O_3$ as the phonon contribution to the specific heat, it is possible to calculate β. The high-temperature β values found without additional fitting parameters agree quite well with the experimental data. This is evidence of the fact that the isotope effect at high temperatures is attributed to the shift in the frequency of optical (oxygen) vibrations. The peak observed at $T < 50$ K evidently results from the vibrations of heavier atoms since the left-hand side of Eq. (2) includes the derivative with respect to the total mass of the unit cell, whereas the changes in the oxygen mass provide only a small contribution to these vibrations.

It is interesting to compare the isotope effect in cobaltites with the results obtained for simpler diatomic compounds. From this viewpoint, the zinc oxide crystal ZnO seems to be the most suitable. The M_O/M ratios for ZnO and $(Pr_{1-y}Eu_y)_{0.7}Ca_{0.3}CoO_3$ are very close to each other. The experimentally determined parameter $\beta_O(T)$ and its values found in the ab initio calculations [10] are shown in Fig. 3. There is a good agreement between the data for ZnO and $(Pr_{1-y}Eu_y)_{0.7}Ca_{0.3}CoO_3$. The temperature dependences of the parameter β for both materials coincide very well. It is quite probable that $\beta_O(T)$ in ZnO correctly describes the contribution of the lattice specific heat to the isotope effect in cobaltites in the entire temperature range. Under such an assumption, the magnetic contribution to the isotope effect can be separated. Upon cooling, $\beta_O(T)$ increases in the samples with a high Eu content. This behavior indicates a fast increase in the magnetic contribution to the specific heat in the samples with the heavier oxygen isotope (see Fig. 2). As a result, the shape of the $\beta_O(T)$ plot is similar to the temperature derivative of the specific heat in the vicinity of the spin-state transition. In the samples with a low Eu content, $\beta_O(T)$ follows the behavior of the lattice isotope parameter for ZnO deviating from it only in the close vicinity of the ferromagnetic transition. In the latter region, $\beta_O(T)$ becomes negative owing to an increase in the magnetic contribution to the specific heat with a decrease in the mass of the oxygen isotope. The magnetic contribution to $\beta_O(T)$ turns out to be large enough to exceed the positive contribution from the lattice specific heat. It is interesting that the isotope effect for the samples with the high Eu content also becomes negative at very low temperatures. This confirms the conclusion drawn in [8] that a certain amount of the ferromagnetic phase exists even in the samples with $y = 0.26$, which are far away from the ferromagnetic region of the phase diagram (see Fig. 1).

The $^{16}O \longrightarrow {}^{18}O$ oxygen isotope substitution leads to significant changes in the behavior of the temperature dependence for all of the measured quantities. We observe a pronounced isotope effect for the temperature of the spin-state transition in the insulating region, whereas it is nearly absent in the ferromagnetic phase. However, the oxygen isotope substitution shifts the $T_{SS}(y)$ and $T_{FM}(y)$ phase boundaries in the similar way toward the lower Eu content. This means that the static distortions related to the changes in the average ionic radius $\langle r_A \rangle$ are equivalent to a certain extent to the dynamical lattice distortions manifesting themselves at the isotope substitution. However, the underlying physical mechanisms can be different. An increase in the Eu content leads to the broadening of the t_{2g}–e_g band due to the crystal-field splitting accompanied by the stabilization of the low-spin state. The isotope substitution leads to the narrowing of the effective conduction band. In this case, the narrowing of the e_g band in the ^{18}O-containing samples leads to an increase in the t_{2g}–e_g gap and to the corresponding increase in the spin-state transition temperature T_{SS}. All of these transformations occur at the boundary between the low-spin and intermediate-spin states, where any change in the width W of the band leads to the appreciable shift of the phase equilibrium and thus to the pronounced enhancement of the isotope effect. As a result, the temperature T_{SS} for the samples with

^{18}O turns out to be significantly higher than that for the samples with ^{16}O.

In the LS region of the phase diagram at a low Eu content, the isotope effect is small and has the opposite sign. It is assumed that the ferromagnetic transition is due to the double-exchange interaction and the transition temperature T_{FM} is proportional to the width of the effective conduction band, which decreases at the $^{16}O \longrightarrow {}^{18}O$ oxygen isotope substitution. The corresponding isotope effect is rather weak, because it is associated with itinerant electrons weakly coupled to the lattice, although the band width is renormalized due to the electron–phonon interaction. In contrast to the situation in manganites, the electrical conductivity is high enough on both sides of the ferromagnetic transition to screen the Jahn–Teller distortions of the lattice, which enhance the effect of the oxygen isotope substitution.

In the samples with the high Eu content corresponding to the region with localized electrons, the lattice effects are strong because the spin-state transition is accompanied by the lattice distortions and the increase in the contribution of lattice degrees of freedom leads to a pronounced isotope effect. This is similar to the situation in manganites, where the isotope effect is attributed to the competition between the states of the charge-ordered insulator and the ferromagnetic metal [13].

4. CONCLUSIONS

Using the whole set of the results and according to the phase diagram involving the magnetic and spin-state transitions, we can conclude that the $^{16}O \longrightarrow {}^{18}O$ oxygen isotope substitution shifts the phase boundaries toward a lower Eu content. An increase in the oxygen mass as well as in the Eu content gives rise to an increase in the temperature T_{SS} and to a slight decrease in the temperature T_{FM}. It is reasonable to suggest that an increase in the isotope mass leads to the increased crystal-field splitting of electron levels and to the stabilization of the low-spin state. The effect of oxygen isotope substitution on the specific heat manifests itself in the form of two contributions, lattice and magnetic. The lattice contribution always results in the positive isotope effect. The value and sign of the magnetic contribution are determined by the type of the magnetic transition. An increase in the effective width of the band with the oxygen isotope mass leads to the stabilization of the low-spin state and to the pronounced increase in T_{SS} under the conditions of the insulator-like spectrum of the charge carriers. In contrast, a slight decrease in T_{FM} with an increase in the oxygen isotope mass in the ferromagnetic composition range is likely attributed to the specific features of the double-exchange mechanism, which is efficient on both sides of the transition due to the metallic-like behavior of the conductivity.

ACKNOWLEDGMENTS

This work was supported by the Russian Foundation for Basic Research, project nos. 07-02-00681, 07-02-91567, and 10-02-00598, and by Deutsche Forschungsgemeinschaft, grant no. 436 RUS113/942/0. We are grateful to A.V. Inyushkin for his assistance and helpful discussions.

REFERENCES

1. N. A. Babushkina, L. M. Belova, O. Yu. Gorbenko, et al., Nature **391**, 159 (1998).
2. C. Zobel, M. Kriener, D. Bruns, et al., Phys. Rev. B **66**, 020402(R) (2002).
3. M. Kriener, C. Zobel, A. Reichl, et al., Phys. Rev. B **69**, 094417 (2004).
4. J. Baier, S. Jodlauk, M. Kriener, et al., Phys. Rev. B **71**, 014443 (2005).
5. S. Tsubouchi, T. Kyomen, and M. Itoh, Phys. Rev. B **69**, 144406 (2004).
6. G. Y. Wang, T. Wu, X. G. Luo, et al., Phys. Rev. B **73**, 052404 (2006).
7. G. Y. Wang, X. H. Chen, T. Wu, et al., Phys. Rev. B **74**, 165113 (2006).
8. A. V. Kalinov, O. Yu. Gorbenko, A. N. Taldenkov, et al., Phys. Rev. B **81**, 134427 (2010).
9. K. Knížek, J. Hejtmánek, Z. Jirák, et al., Phys. Rev. B **79**, 134103 (2009).
10. J. Serrano, R. K. Kremer, M. Cardona, et al., Phys. Rev. B **73**, 094303 (2006).
11. R. K. Kremer, M. Cardona, E. Schmitt, et al., Phys. Rev. B **72**, 075209 (2005).
12. M. Cardona, R. K. Kremer, R. Lauck, et al., Phys. Rev. B **76**, 075211 (2007).
13. N. A. Babushkina, A. N. Taldenkov, A. V. Inyushkin, et al., Phys. Rev. B **78**, 214432 (2008).

Translated by R. Tyapaev